Taylor & Francis
Taylor & Francis Group

CLINICAL STUDY

Check for updates

DKK3 promotes renal fibrosis by increasing MFF-mediated mitochondrial dysfunction in Wnt/β-catenin pathway-dependent manner

Jianling Song, Yanxia Chen, Yan Chen, Minzi Qiu, Wenliu Xiang, Ben Ke and Xiangdong Fang

Department of Nephrology, The Second Affiliated Hospital, Jiangxi Medical College, Nanchang University, Nanchang, Jiangxi Province, P.R. China

ABSTRACT

Background: Chronic kidney disease (CKD) lacks effective treatments and renal fibrosis (RF) is one of CKD's outcomes. Dickkopf 3 (DKK3) has been identified as an agonist in CKD. However, the underlying mechanisms of DKK3 in CKD are not fully understood.

Methods: H_2O_2-treated HK-2 cells and ureteric obstruction (UUO) mice were used as RF models. Biomarkers, Masson staining, PAS staining, and TUNEL were used to assess kidney function and apoptosis. Oxidative stress and mitochondria function were also evaluated. CCK-8 and flow cytometry were utilized to assess cell viability and apoptosis. Western blotting, IHC, and qRT-PCR were performed to detect molecular expression levels. Immunofluorescence was applied to determine the subcellular localization. Dual luciferase assay, MeRIP, RIP, and ChIP were used to validate the m6A level and the molecule interaction.

Results: DKK3 was upregulated in UUO mouse kidney tissue and H_2O_2-treated HK-2 cells. Knockdown of DKK3 inhibited oxidative stress, maintained mitochondrial homeostasis, and alleviated kidney damage and RF in UUO mice. Furthermore, DKK3 silencing suppressed HK-2 cell apoptosis, oxidative stress, and mitochondria fission. Mechanistically, DKK3 upregulation was related to the high m6A level regulated by METTL3. DKK3 activated TCF4/β-catenin and enhanced MFF transcriptional expression by binding to its promoter. Overexpression of MFF reversed in the inhibitory effect of DKK3 knockdown on cell damage.

Conclusion: Upregulation of DKK3 caused by m6A modification activated the Wnt/β-catenin pathway to increase MFF transcriptional expression, leading to mitochondrial dysfunction and oxidative stress, thereby promoting RF progression.

Introduction

The incidence of chronic kidney disease (CKD) is increasing year by year, and a large-scale epidemic survey in 2012 shows that the incidence of CKD in China has reached about 10.8% [1]. Renal fibrosis (RF) is one of the common pathological manifestations when CKD progresses to end-stage renal disease (ESRD) [2]. Current studies have shown that the degree of renal interstitial fibrosis damage is more effective than the degree of glomerular damage in predicting renal dysfunction [3]. Oxidative stress not only causes glomerulosclerosis but also affects renal tubules, resulting in renal tubular filtration disorders and tubular interstitial fibrosis [4]. Therefore, elucidating the mechanism of oxidative stress in

RF is essential for designing targeted drugs alleviating kidney damage.

Mitochondria are a class of highly plastic and dynamic organelles that can adapt to a variety of stress conditions. Mitochondria are very sensitive under pathological conditions [2,5]. When mitochondrial dysfunction occurs, damaged renal tubular epithelial cells undergo phenotypic transformation, disrupting normal tubular interstitial structure and leading to interstitial inflammation and fibrosis [6,7]. Improving mitochondrial dynamics plays a key role in alleviating RF and delaying CKD progression. In mammalian cells, mitochondrial fission factor (MFF) is a crucial component for Drp1 recruitment to the mitochondria during mitochondrial fission [8]. The transcription of fibrosis-related genes was epigenetically

regulated by Drp1-mediated mitochondrial fission, thereby promoting the activation and proliferation of renal fibroblast [9]. However, the function of MFF in RF has not been well characterized.

Dickkopf 3 (DKK3) is an upstream regulator of the Wnt signaling pathway. As reported, knockout of DKK3 caused tubular atrophy and decreased interstitial matrix accumulation in RF mice, which was associated with the weakening of the Wnt/catenin pathway [10]. Furthermore, DKK3, as a stimulant of the Wnt pathway, can antagonize the role of DKK1 in the transformation of fibroblasts to myofibroblasts, and promote the transformation of myofibroblasts and endothelial-mesenchymal [11]. Clinically relevant evidence also suggested that DKK3 was an effective biomarker for CKD [12,13]. Additionally, it has been shown that DKK3 may be involved in the regulation of mitochondrial function [14–16]. In human ovarian cancer cells, DKK3 caused apoptosis *via* the mitochondria-related pathways [15]. DKK3 has been observed to trigger apoptosis in human colon cancer plausibly *via* the mitochondrial pathway [16]. Previous study also revealed that miR-25 regulated Wnt/β-catenin signaling pathway by targeting DKK3 [17]. Bioinformatics analysis found that there may be a potential transcriptional regulatory relationship between the TCF4/β-catenin complex and MFF promoter. Therefore, DKK3 may regulate MFF-mediated mitochondrial dysfunction in RF through β-catenin signaling, which needs further study.

N^6-methyladenosine (m6A) modification affects RNA processing, stability, transport, and translation, thereby regulating gene expression and function [18]. Methyltransferase-like 3 (METTL3) is a key component of the mammalian N6-adenine methyltransferase complex and acts as an encoder for m6A methylation [19]. m6A modification and METTL3 are also related to mitochondrial homeostasis. METTL3 decreased the stability of PGC-1α mRNA *via* enhanced m^6A methylation and promoted mitochondrial dysfunction [20]. Additionally, m6A modification participated in the occurrence and development of RF by affecting the proliferation, differentiation, migration, and apoptosis of different types of cells in the kidney [21]. METTL3 activated renal interstitial fibroblasts by promoting the maturation of miR-21-5p, and enhanced inflammation through SPRY1/ERK/NF-κB signaling pathway [18]. However, the related studies remained limited. We found multiple m6A modification sites on DKK3 through the SRAMP database (http://www.cuilab.cn/sramp). Based on the above information, we hypothesize that METTL3 might mediate m6A modification of DKK3 and alter its expression.

We aimed to investigate how DKK3 affected mitochondrial homeostasis and RF development. Our study showed that the abnormal upregulation of DKK3 was due to METTL3-mediated m6A modification, which then activated MFF transcription and caused mitochondrial dysfunction as well as exacerbated RF. DKK3-mediated mitochondrial dysfunction is a new molecular mechanism of RF occurrence, and targeted inhibition of DKK3 has emerged as a novel therapeutic target for RF.

Materials and methods

Construction of UUO mouse model

4-6 week-old C57BL/6J male mice were purchased from Hunan SJA Laboratory Animal Co., Ltd. Mice were assigned to four groups: sham, UUO, UUO + shNC, and UUO + shDKK3. Each group had six animals. The mice were weighed and anesthetized by intraperitoneal injection. Ophthalmic scissors were used to cut a longitudinal incision of about 1 cm at 0.5 cm on the left side of the spine and 0.5 cm at the lower edge of the left costal arch, and the left thumb and index finger were used to gently squeeze out the left kidney. The ureter can be seen at the lower pole of the left kidney. The poles were ligated with 3-0 silk threads, and the distance between the two ligatures was greater than 0.5 cm [22]. For the sham group, the operation was the same except for the ligation process. This experiment was approved by the Animal Ethics Committee of the Second Affiliated Hospital of Nanchang University and strictly followed animal ethics. Mice were given either 2×10^7 Pfu Lv-shDKK3 (200 μL) or shNC (200 μL) twice weekly intravenously for 24 h following UUO surgery [23]. Each mouse's kidney and serum were collected at the end of the trial. The sequence of shDKK3 and shNC was listed here: 5′-AGCCATGAATGTATCATTGAT-3′ (shDKK3) and 5′-GTTCTCC GAACGTGTCACGT-3′(shNC).

Measurements of serum creatinine (Cr) and blood urea nitrogen (BUN)

Serums of sham or UUO mice were collected and kits from Shanghai Enzyme-linked Biotechnology Co., Ltd. (Shanghai, China) were used to detect Cr and BUN levels according to the instructions.

HE staining

The kidney tissue was fixed in 4% paraformaldehyde. Slices of the paraffin-coated kidney samples were taken. 5 μm paraffin sections were dewaxed using a seines of ethanol. The sections were subjected to sequential immersion in xylene I/II, absolute ethanol I/II, and 75% alcohol for durations of 20, 5, and 5 min, respectively, and subsequently rinsed with water. Subsequently, the sections were subjected to hematoxylin staining (Servicebio, Wuhan, China) for a duration of 3–5 min. Following sequential dehydration in 85% and 95% alcohol, the sections were subjected to staining with an eosin staining solution (Servicebio, Wuhan, China) for a duration of 5 min. Subsequently, the process of dehydration and sealing was executed, followed by the acquisition of images utilizing a light microscope. Scores on the HE staining for interstitial dilatation and inflammatory cell infiltration ranged from 0 to 5. 0: normal; 1: <10% positive; 2: 10–25% of tubules injured area positive; 3: 25–50% positive; 4: 50–75% positive; 5: >75% positive [24].

Masson staining

The kidney tissue was fixed in 4% paraformaldehyde. Slices of the paraffin-coated kidney samples were taken. Masson's Trichrome Stain Kit (Servicebio, Wuhan, China) was used on kidney tissues. Subsequently, thin sections measuring 5 μm were subjected to staining procedures involving potassium dichromate, iron hematoxylin, ponceau acid fuchsin, phosphomolybdic acid, and aniline blue solution, respectively. The slices were differentiated with 1% glacial acetic acid and then dehydrated with ethanol. A total of five fields of view were selected at random from each section under the light microscope. The Masson staining was utilized to semi-quantitatively analyze the collagen volume fraction, which is defined as the proportion of collagen-positive blue area to the total tissue area. The Image J software was employed for this purpose.

PAS staining

A PAS stain kit (Servicebio, Wuhan, China) was used to perform PAS staining. The dewaxing process was described above. Then, sections were stained in periodic acid solution, Schiff solution, and hematoxylin solution, respectively. The observation was performed under the light microscope.

TUNEL assay

After dewaxing, endogenous peroxidase inhibition, and antigen retrieval, TUNEL staining was performed using a TUNEL detection kit (Roche, Switzerland). Subsequently, the slides underwent immersion in a solution containing hydrogen peroxide and streptavidin-horseradish peroxidase. After adding a solution of 3,3-diaminobenzidine tetrachloride, the TUNEL-stained cells were observed using an optical microscope. The number of TUNEL-positive cells was analyzed using ImageJ software.

IHC

Kidney tissue sections were blocked after dehydration, dewaxing, and antigens repair. Then the sections were incubated using primary antibody Drp1 (ab184247, Abcam, Cambs, UK), and 4-HNE (ab48506, Abcam, Cambs, UK) at 4 °C overnight and then secondary antibodies were added. The sections were then washed with PBS and DAB was added. Hematoxylin was used to depict the nucleus. Brown was the positive staining area, and 5 nonoverlapping fields of view were randomly collected under light microscopy per section, and the positive staining area was measured.

Cell culture and treatment

HK-2 cells (Procell Life Science & Technology Co., Ltd., Wuhan, China) were placed in DMEM medium (Gibco, CA, USA) containing 10% fetal bovine serum, 1% penicillin/streptomycin, and were incubated at 37 °C in the incubator with 5% CO_2.

Cell growth was observed under an inverted microscope. When the cell growth and fusion coverage reaches 75%–85%, routinely digest and passage with 0.25% trypsin (1:2 or 1:3). Wnt inhibitors LF3 was diluted in DMSO to a working concentration of 2 μM. Following 24 h incubation, HK-2 cells were treated with or without H_2O_2 (500 μM) and LF3 for 48 h [25]. The STM2457 (HY-134836) was purchased from MCE (Shanghai, China).

Cell transfection

Short hairpin RNA targeting DKK3 (shDKK3, 5'-GCCACC CTCAATGAGATGTTC-3') and scramble shRNA controls (shNC, 5'-CGTACGCGGAATACTTCGA-3') were generated by Shanghai GenePharma (Shanghai, China). The coding sequences of TCF4, β-catenin, METTL3, and MFF were amplified from human cDNA and integrated into pcDNA 3.1 to generate overexpression plasmids. Lipofectamine 3000 (Thermo Fisher Scientific) was used for transfection into cells. The final concentration was 20 μM for shRNA and 20 μg for the plasmids. Cells were harvested 48 h after the transfection. Additionally, shDKK3 or shNC was cloned into the lentiviral vector pLKO.1, and lentiviral particles were packaged in 293T cells. After 48-h culture, the cell supernatant was collected, and the lentivirus obtained after centrifugation, filtration, and concentration were used for subsequent experiments. 2 μg/mL of puromycin was added to the culture plate for drug screening. After 96 h, the cells were observed, and photographed, the surviving cells were collected and purified, and the mRNA expression of the target gene was detected by qRT-PCR. The stable cell line was cryopreserved for subsequent experiments.

RNA extraction and qRT-PCR

Total RNA was extracted from tumor tissues and cell lines using TRIzol® reagent (Thermo Fisher Scientific, MA, USA). The assessment of RNA quality was conducted using NanoDrop™ 2000 Spectrophotometers (Thermo Fisher Scientific, MA, USA). The optimal OD260/280 range for RNA of sufficient quality is between 1.8 and 2.0. Subsequently, the RNA specimens were employed to generate complementary DNA (cDNA) utilizing the PrimeScriptTM RT reagent Kit (Takara, Dalian, China). qRT-PCR was used to determine the gene expression of DKK3, METTL3 and MFF using SYBR® Green Real-Time PCR master mix (Thermo Fisher Scientific, MA, USA) on ABI StepOnePlusTM Real-Time PCR System (Applied Biosystems, CA, USA). Each specimen underwent three evaluations. The reference genes utilized in the study were β-actin, and the primer sequences for the tested genes are presented in Table 1.

Western blotting

Total protein was extracted by lysing cells in RIPA buffer (Servicebio, Wuhan, China) supplemented with protease

Table 1. Primers used for qRT-PCR analysis.

Genes	Primer sequences (5′–3′)
mDKK3-F	TTGCTGACATTCTGTTGACCC
mDKK3-R	TCGGTCCAAAGCTCCTTCAG
hDKK3-F	TATGTGTGCAAGCCGACCTT
hDKK3-R	AAAGCACACACCTGGGGAAA
METTL3-F	GAGTGCATGAAAGCCAGTGA
METTL3-R	CTGGAATCACCTCCGACACT
MFF-F	GCTCTCAGCCAACCACCTC
MFF-R	GGAGAAGGAAATGCTGCCCT
β-actin-F	CCCTGGAGAAGAGCTACGAG
β-actin-R	CGTACAGGTCTTTGCGGATG

inhibitors (Beyotime, Shanghai, China). Mouse kidney tissues were collected and pulverized using a mortar in RIPA buffer containing protease inhibitors to obtain the total protein extract. The protein of equal quantity was segregated and subsequently transferred onto a polyvinylidene difluoride (PVDF) membrane (Invitrogen, NY, USA). Subsequently, the sample was subjected to blocking in Tris Buffered Saline Tween (TBST) containing 5% skim milk powder. Subject the membrane to primary antibody including α-SMA (#14968, Cell Signaling Technology, MA, USA), E-cadherin (#14472, Cell Signaling Technology), Fibronectin (#26836, Cell Signaling Technology), TGF-β (#3711, Cell Signaling Technology), DKK3 (ab187532, Abcam), Mfn2 (#9482, Cell Signaling Technology), MFF (#86668, Cell Signaling Technology), Drp1 (#8570, Cell Signaling Technology), YME1L (ab170123, Abcam, Cambs, UK), NOX4 (ab154244, Abcam), Bax (#2772, Cell Signaling Technology), Bcl2 (#3498, Cell Signaling Technology), Cleaved-caspase 3 (#9661, Cell Signaling Technology), Caspase 3 (#9662, Cell Signaling Technology), METTL3 (#86132, Cell Signaling Technology), β-Tubulin (internal control of α-SMA and TGF-β, #2146, Cell Signaling Technology) and β-actin (internal control for other proteins, #93473, Cell Signaling Technology) at 4 °C overnight. Subsequently, the membrane was subjected to three rounds of TBST washes at 5 min intervals, followed by incubation with HRP-conjugated secondary antibody (1:2000, Abcam, Cambridge, UK) at room temperature for a duration of 2 h. Following the washing process, the bands were captured through the employment of the Gel Imaging System (Life Science, CA, USA). Subsequently, the intensity of the bands was analyzed using the ImageJ software.

Chromatin immunoprecipitation (ChIP)

The protein and chromatin in the cells were cross-linked with formaldehyde, the nuclear membrane was disrupted by ultrasonic three times. Then, the DNA concentration was measured, and the size of DNA fragments was determined by 1% agarose gel electrophoresis. 1:50 diluted TCF4 (ab217668, Abcam, Cambs, UK) or β-catenin (ab32572, Abcam, Cambs, UK) antibody and negative control antibody IgG were added to the samples, and samples were incubated overnight at 4 °C. Chromatin was eluted from protein and de-cross-linked by ChIP buffer and magnetic beads, DNA was purified by spin column, and the purified DNA was subjected to qRT-PCR.

Dual-luciferase reporter assays

The putative binding sites with TCF4 or β-catenin in the MFF promoter were amplified and cloned into the pGL3 vectors (Promega, Madison, WI, USA) using partial sequences. Subsequently, pGL3 vectors were co-transfected into HK-2 cells with TCF4 or β-catenin overexpression vector. Following a 48 h transfection period, cellular lysis was performed and luciferase activity was measured using a microplate reader following the guidelines provided by the dual-luciferase reporter gene detection kit (Beyotime, Shanghai, China).

RNA immunoprecipitation assay

The Magna RIP Kit (Millipore, Bedford, MA, USA) was utilized to perform RIP assays. In brief, the cells were collected and subjected to lysis using a lysis buffer. Subsequently, the lysates were subjected to incubation with magnetic beads that had been conjugated by an m6A (ab208577, Abcam, Cambs, UK)/METTL3 antibody (#86132, Cell Signaling Technology, MA, USA) or negative control normal mouse IgG (#3900, Cell Signaling Technology, MA, USA). The products that underwent immunoprecipitation were subjected to purification, and subsequently, the presence of DKK3 was assessed through qRT-PCR.

CCK-8 assay

HK-2 cells in the logarithmic growth phase were seeded in a 96-well culture plate and allowed to adhere for 24 h. After a 72-h incubation period, 10 microliters of CCK-8 detection solution were introduced into each well. The optical density of each well was measured at a wavelength of 450 nm for statistical analysis.

Detection of apoptosis rate by flow cytometry

HK-2 cells were trypsinized without EDTA, centrifuged, resuspended in PBS and counted. Two hundred microliters of Annexin V-FITC (BD, USA) binding solution was added to resuspended cells at a cell density of 1×10^6 cells/mL. The cells were subjected to a 10-min incubation period at ambient temperature under conditions of low light. A mixture was prepared by combining 190 μL of Annexin V-FITC binding solution with 10 μL of propidium iodide (PI) staining solution and was placed on ice in the dark for 15 min. Then apoptosis signals were detected by flow cytometer (BD, CA, USA).

Mitochondrial membrane potential detection

JC-1 working solution was prepared according to the JC-1 mitochondrial membrane potential detection kit (Beyotime, Shanghai, China). The diluted JC-1 working solution was added to the purified mitochondria (9:1 by volume), and fluorescent enzyme labeling was used. The instrument detected the JC-1 monomer and dimer.

Oxidative stress indicator detection

Cells were grouped according to the different experiment designs. MitoSOX (M36008, Thermo Fisher, MO, USA), malondialdehyde (MDA) (S0131S, Betotime, Shanghai, China), superoxide sismutase (SOD) (S0101S, Beyotime), and glutathione peroxidase (GPX) (S0056, Beyotime) were detected by corresponding reagents used. Briefly, the cell medium was removed, and a working solution was added. After incubation, the signal was detected under the fluorescence microscope or microplate reader.

ATP activity assay

The quantification of ATP was carried out by employing an ATP detection kit (Solarbio, Beijing, China). A volume of 100 microliters of ATP test working solution was introduced into the 96-well plate, followed by an incubation period at a specified temperature lasting between 3 to 5 min. Following the depletion of background ATP, a volume of 20 μL of either sample or standard was promptly introduced and thoroughly blended. The microplate reader was used to capture signals.

Statistical analysis

All experiments were repeated more than three times. Data were presented as the mean ± standard deviation (SD). The data were analyzed using GraphPad Prism 7, a software developed by GraphPad Software Inc. The statistical analysis employed for comparing two groups was the unpaired two-tailed Students' *t*-test. For multiple groups, the One-way analysis of variance (ANOVA) was utilized, followed by the Tukey *post hoc* test. The threshold for statistical significance was established as $p < 0.05$.

Results

Knockdown of DKK3 alleviated renal injury and fibrosis in UUO mice

Mice were exposed to UUO operation and then treated with or without shDKK3. Fluorescence images showed that shRNAs were successfully delivered into mice kidney tissues (Figure S1). The results of IHC and Western blotting showed that the expressions of mitochondrial fission biomarker Drp1 in the kidney tissue of the UUO group were upregulated, and knockdown of DKK3 could significantly repress Drp1 expression (Figure 1(A&B)). Additionally, the serum levels of CR and BUN in the UUO group were increased compared with the sham group, and DKK3 silencing significantly suppressed this trend (Figure 1(C&D)). HE and Masson staining revealed that compared with the sham-operated group, the UUO group had obvious renal fibrosis features such as renal tubular atrophy or collapse, enlarged renal tubular lumen, renal tubular partially atrophied, increased mesangial cells, and diffuse inflammatory cell infiltration in the mesangial stroma. PAS staining showed dilatation of the renal tubules, mesangial

inflammatory cell infiltration and vacuolated renal tubular epithelial cell changes in UUO mice. Some renal tubular epithelial cells may be necrotic and detached into the lumen, and tubular pattern was rare. These pathological changes were significantly ameliorated by DKK3 knockdown (Figure 1(E–G)). Moreover, fibrosis-related factors α-SMA, E-cadherin, Fibronectin and transforming growth factor β (TGF-β) were detected by Western blotting. Compared with the sham group, the contents of fibrosis factors α-SMA, Fibronectin, and TGF-β were increased, while the expression of epithelial marker factor E-cadherin was decreased (Figure 1(H)). DKK3 silencing significantly reversed the expression changes of these proteins (Figure 1(H)). Notably, the cell apoptosis rate in the UUO group was significantly increased, while the apoptosis rate was decreased after DKK3 silencing (Figure 1(I)). Finally, DKK3 was detected by qRT-PCR and Western blotting. Compared with UUO + shNC group, the mRNA and protein levels of DKK3 in UUO + shDKK3 group were significantly decreased, indicating that shDKK3 could significantly inhibit DKK3 expression in mouse kidney tissue (Figure 1(J&K)). The above results indicated that DKK3 silencing greatly improved renal injury and renal fibrosis in UUO mice.

Knockdown of DKK3 suppressed oxidative stress and maintained mitochondrial homeostasis in UUO mice

Mice were exposed to UUO operation and then treated with or without shDKK3, and the biomarkers of oxidative stress and mitochondria status were examined. Immunohistochemical detection showed that the expressions of oxidative stress biomarker 4-HNE in the kidney tissue of the UUO mice were upregulated, and knockdown of DKK3 reversed this trend (Figure 2(A)). DKK3 silencing inhibited the increase of MDA and the decrease of SOD and GPX in UUO mice kidney tissue (Figure 2(B–D)). The expression of the mitochondrial fusion-related proteins Mfn2 and YME1L in UUO mice kidney tissue was lower than that of the sham group, but the expression of NOX4 and the mitochondrial fission-related proteins MFF and Drp1 was higher (Figure 2(E)). The alterations in these proteins were also reversed by DKK3 silencing (Figure 2(E)). The ATP content in UUO mice kidney tissues was lower than that in the sham group, and this result was considerably reversed by DKK3 silencing (Figure 2(F)). The research mentioned above demonstrated that DKK3 silencing reduced oxidative stress and preserved mitochondrial homeostasis in RF mice.

Knockdown of DKK3 inhibited H₂O₂-induced cell apoptosis and fibrosis in HK-2 cells

To test the function of DKK3 in renal tubular epithelial cells, HK-2 cells were transfected with shDKK3 and treated with H_2O_2. H_2O_2 treatment considerably increased the expression of DKK3 compared to control group, whereas shDKK3 dramatically lowered the expression of DKK3 (Figure 3(A&B)). H_2O_2 treatment dramatically reduced cell viability, whereas DKK3 silencing restored cell vitality (Figure 3(C)). After DKK3
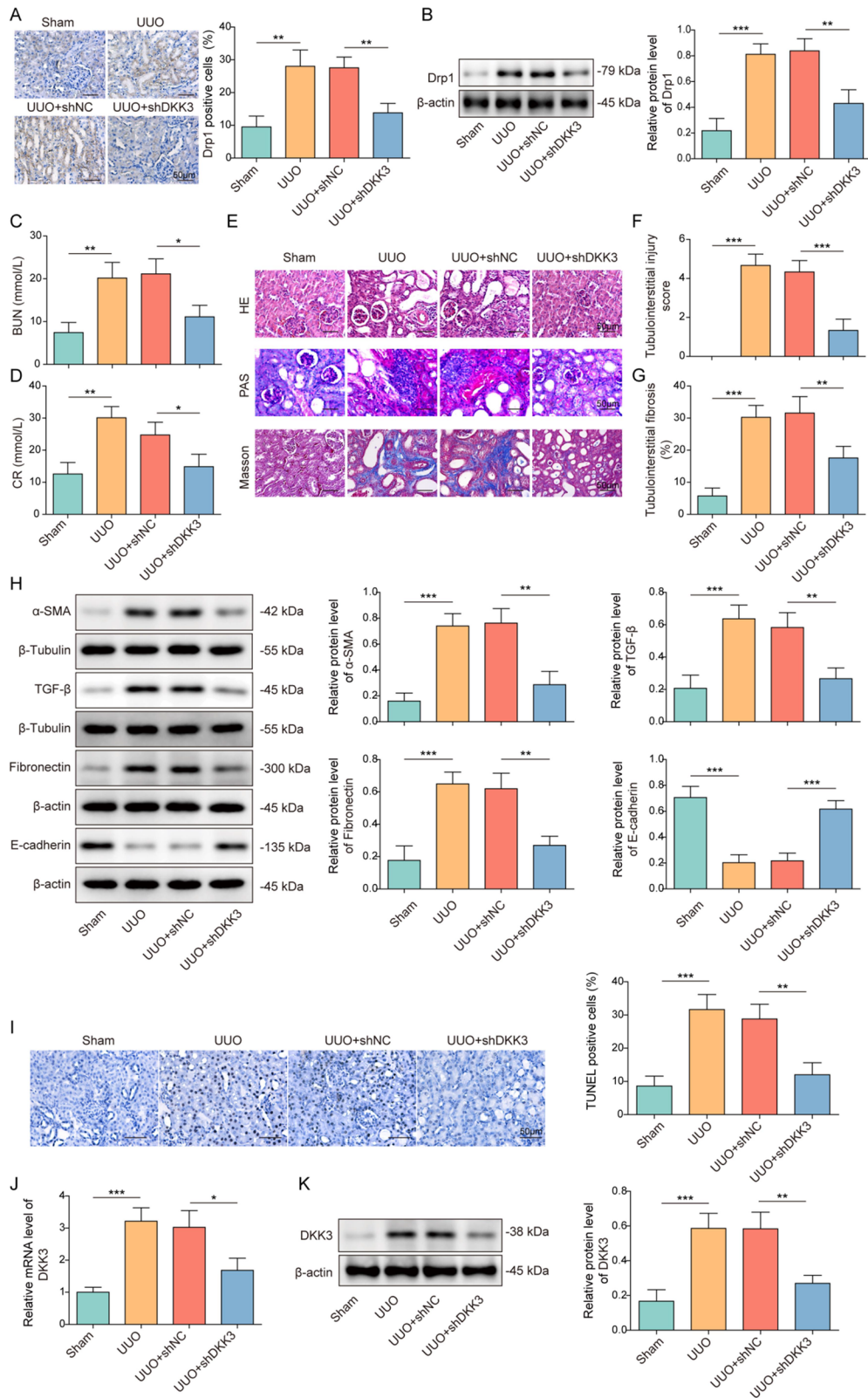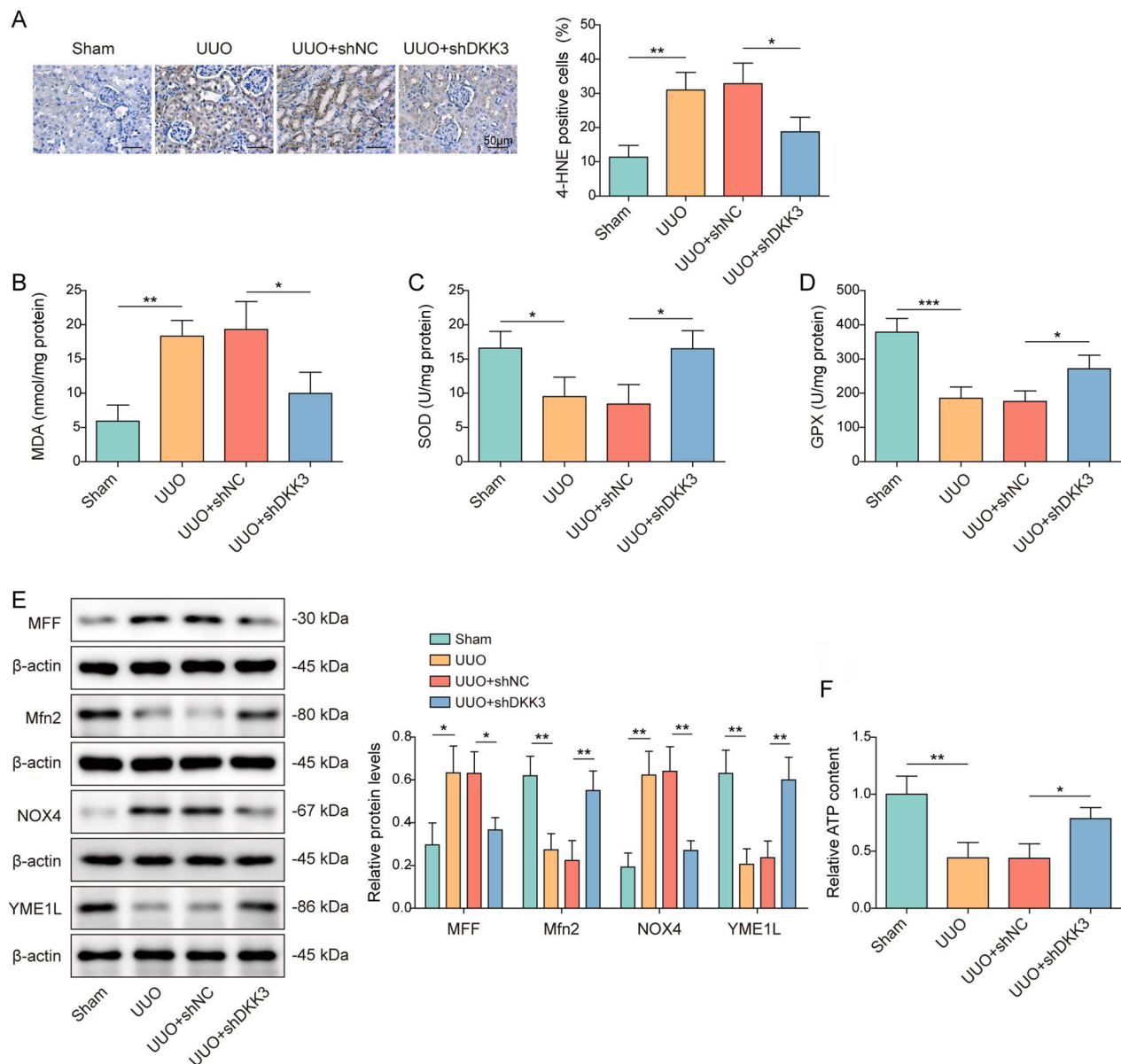
Figure 1. Knockdown of DKK3 alleviated renal injury and renal fibrosis in UUO mice. C57BL/6J mice were exposed to sham or UUO operation and UUO mice were treated with or without shDKK3. Each group had 6 mice. A&B. The protein level of Drp1 was detected by IHC and Western blotting, respectively. C. Serum CR level was measured by CR assay kit. D. Serum BUN level was measured by Urea Assay Kit. E–G. HE staining, Mason staining and PAS staining of mice kidney tissue in each group were detected. Scale bar, 50 μm. H. α-SMA, Fibronectin, TGF-β and E-cadherin in kidney tissue were measured by Western blotting. I. The apoptosis level was evaluated by TUNEL assay. Scale bar, 50 μm. J&K. The mRNA and protein expression of DKK3 were detected by qRT-PCR and Western blotting, respectively. Data were presented as mean ± SD. *$p < 0.05$, **$p < 0.01$ and ***$p < 0.001$.

Figure 2. Knockdown of DKK3 suppressed oxidative stress and maintained mitochondrial homeostasis in UUO mice. C57BL/6J mice were exposed to sham or UUO operation and UUO mice were treated with or without shDKK3. Each group had 6 mice. A. 4-HNE was detected by IHC in each group. Scale bar, 50 μm. B. MDA was detected by the assay kit. C. SOD was detected by the assay kit. D. GPX was detected by the assay kit. E. The protein expressions of Mfn2, MFF, Drp1, YME1L and NOX4 in kidney tissue were measured by Western blotting. F. ATP content was detected in kidney tissues by the assay kit. Data were expressed as mean ± SD. *$p < 0.05$, **$p < 0.01$ and ***$p < 0.001$.

silencing, the trend of increased apoptosis induced by H_2O_2 treatment was considerably reversed (Figure 3(D)). Apoptosis markers Bax, Bcl2, cleaved-caspase 3, and caspase 3 were detected by Western blotting. H_2O_2 treatment reduced Bcl2 expression, but boosted Bax and cleaved-caspase 3 expression (Figure 3(E)). The changing trend of these apoptosis-related proteins was considerably weakened by DKK3 silencing (Figure 3(E)). Furthermore, H_2O_2 treatment increased the content of fibrotic factors α-SMA, Fibronectin, and TGF-β, while decreased the expression of epithelial marker factor E-cadherin (Figure 3(F)). DKK3 silencing significantly reversed the expression changes of these proteins (Figure 3(F)). The above results indicated that inhibiting DKK3

function in HK-2 cells prevented H_2O_2-induced apoptosis and fibrosis.

Knockdown of DKK3 repressed H_2O_2-induced oxidative stress and mitochondrial fission

The oxidative stress and mitochondria status were also examined in the cell model. Mitochondrial ROS content was detected by mitoSOX and the result presented that H_2O_2 administration significantly boosted the generation of mitochondrial ROS, but DKK3 silencing reversed this tendency (Figure 4(A)). The inhibitory effects on SOD and GPX enzyme activity and increasing on MDA expression of H_2O_2 treatment
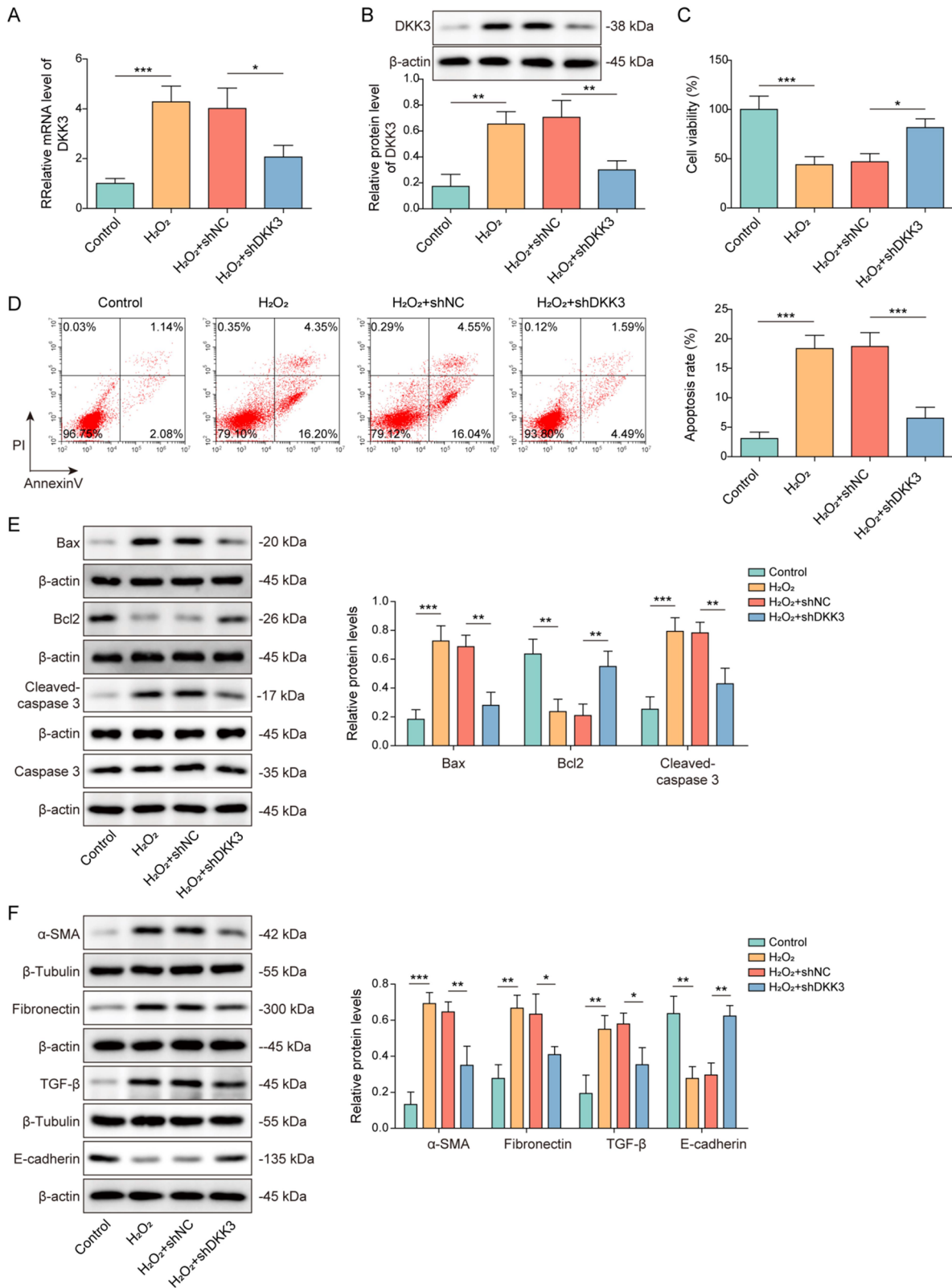
Figure 3. Knockdown of DKK3 inhibited H_2O_2-induced cell apoptosis and fibrosis in HK-2 cells. HK-2 cells transfected with shNC or shDKK3 were then treated with saline (control group) or 500 μM H_2O_2 for 48 h. A. The mRNA expression of DKK3 was detected by qRT-PCR. B. The protein expression of DKK3 was detected by Western blotting. C. Cell viability was examined by CCK-8 assay kit. D. Cell apoptosis was assessed by flow cytometry. E. The protein expressions of Bax, Bcl2, Cleaved-caspase 3 and Caspase 3 in HK-2 cells were measured by Western blotting. F. The protein expressions of α-SMA, Fibronectin, TGF-β and E-cadherin in HK-2 cells were measured by Western blotting. Data were presented as mean ± SD. *$p < 0.05$, **$p < 0.01$ and ***$p < 0.001$.
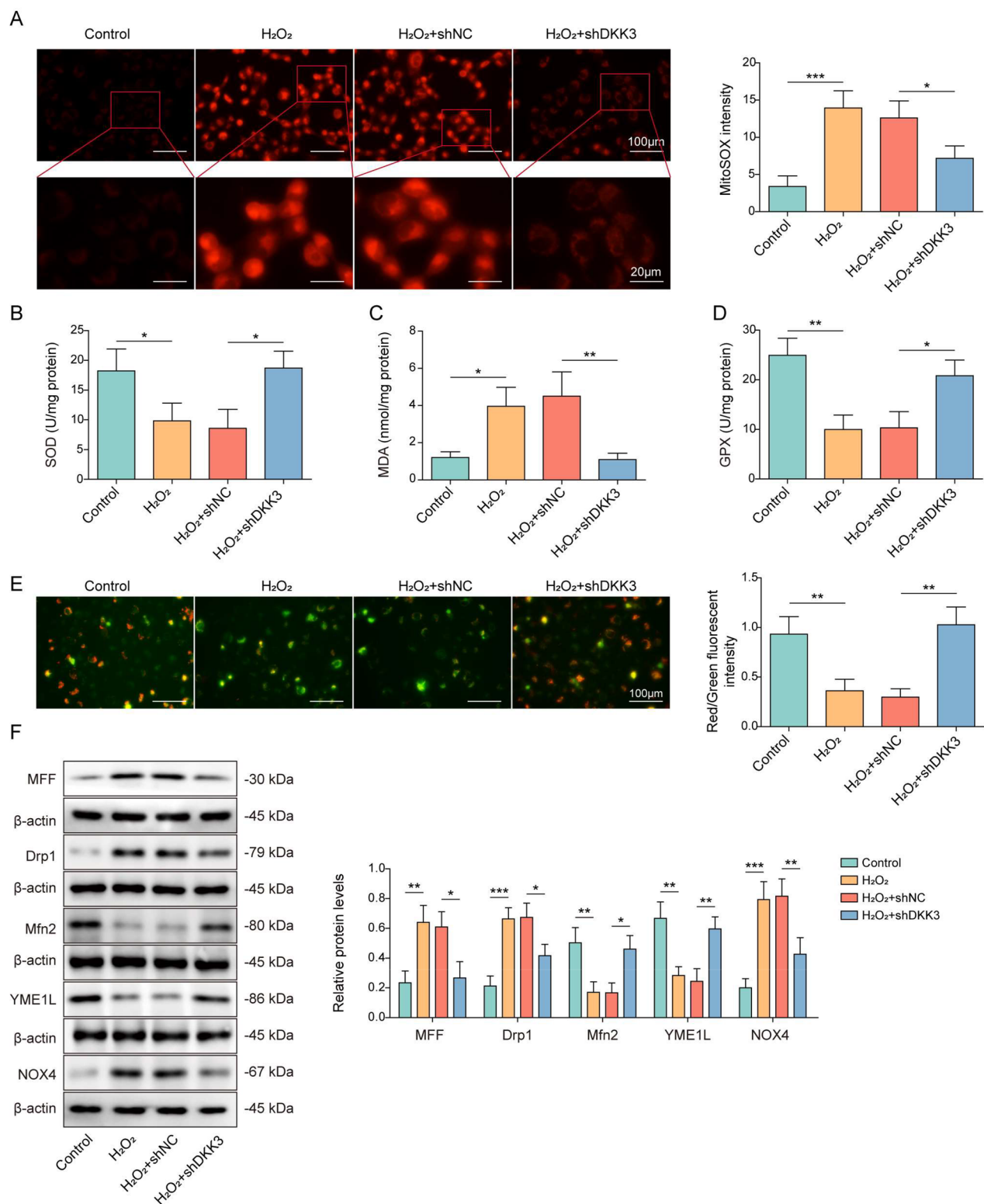
Figure 4. Knockdown of DKK3 repressed H_2O_2-induced oxidative stress and mitochondrial fission. HK-2 cells transfected with shNC or shDKK3 were treated with saline (control group) or 500 μM H_2O_2 for 48 h. A. Mitochondria ROS level was measured by mitoSOX assay kit. Scale bar, 100 μm and 20 μm. B. SOD was detected by the assay kit. C. MDA was detected by the assay kit. D. GPX was detected by the assay kit. E. Mitochondrial membrane potential was measured by JC-1 detection kit. F. The protein expressions of Mfn2, MFF, Drp1, YME1L and NOX4 in HK-2 cells were measured by Western blotting. Data were expressed as mean ± SD. $*p < 0.05$, $**p < 0.01$ and $***p < 0.001$.

were evident when compared to control group, but these effects were restored following DKK3 silencing (Figure 4(B–D)). Mitochondrial membrane potential was suppressed after

H_2O_2 administration, but DKK3 silencing reversed this inhibitory effects (Figure 4(E)). Furthermore, Mfn2 and YME1 were decreased in the H_2O_2 group, whereas MFF, Drp1, and NOX4

were increased (Figure 4(F)). The biological alterations of these proteins were considerably undone by DKK3 silencing (Figure 4(F)). Collectively, these results suggested that DKK3 silencing reduced oxidative damage and mitochondrial fission caused by H_2O_2.

Upregulation of DKK3 was associated with METTL3-mediated m6A modification

The mechanisms of aberrant DKK3 upregulation were then explored. Analysis of DKK3's m6A modification sites using the SRAMP database revealed that DKK3 mRNA contained several m6A binding sites (Figure 5(A)). H_2O_2 treatment raised the amount of m6A alteration on the DKK3 mRNA. (Figure 5(B)). The interaction between METTL3 and DKK3 was detected by RIP. Compared to the IgG group, DKK3 was considerably enriched by METTL3 antibody (Figure 5(C)). Overexpression of METTL3 considerably increased the mRNA and protein levels of METTL3 and DKK3 (Figure 5(D–F)), suggesting that METTL3 promoted DKK3 expression in HK-2 cells. We further validated this using STM2457, a specific inhibitor of METTL3.

The mRNA and protein level expression of DKK3 were significantly downregulated after STM2457 treatment (Figure 5(G&H)). Taken together, DKK3 abnormal upregulation was connected to METTL3-mediated m6A modification.

DKK3 promoted MFF transcription mediated by the TCF4/β-catenin complex

Downstream mechanisms of DKK3 were further studied. β-catenin was visualized by immunofluorescence detection. H_2O_2 overexpression dramatically boosted the expression and nuclear translocation of β-catenin, and this effect was reversed after DKK3 knockdown (Figure 6(A)). Overexpression of the TCF4 and β-catenin both dramatically increase the transcriptional activity of MFF (Figure 6(B)). The interaction was further assessed by ChIP assay. MFF promoter was enriched in TCF4 or β-catenin-pulled complexes (Figure 6(C)). Moreover, overexpression of TCF4 and β-catenin considerably increased the expression of MFF (Figure 6(D&E)). DKK3 overexpression boosted MFF expression, whereas MFF expression was repressed after LF3 (a TCF4 and β-catenin interaction
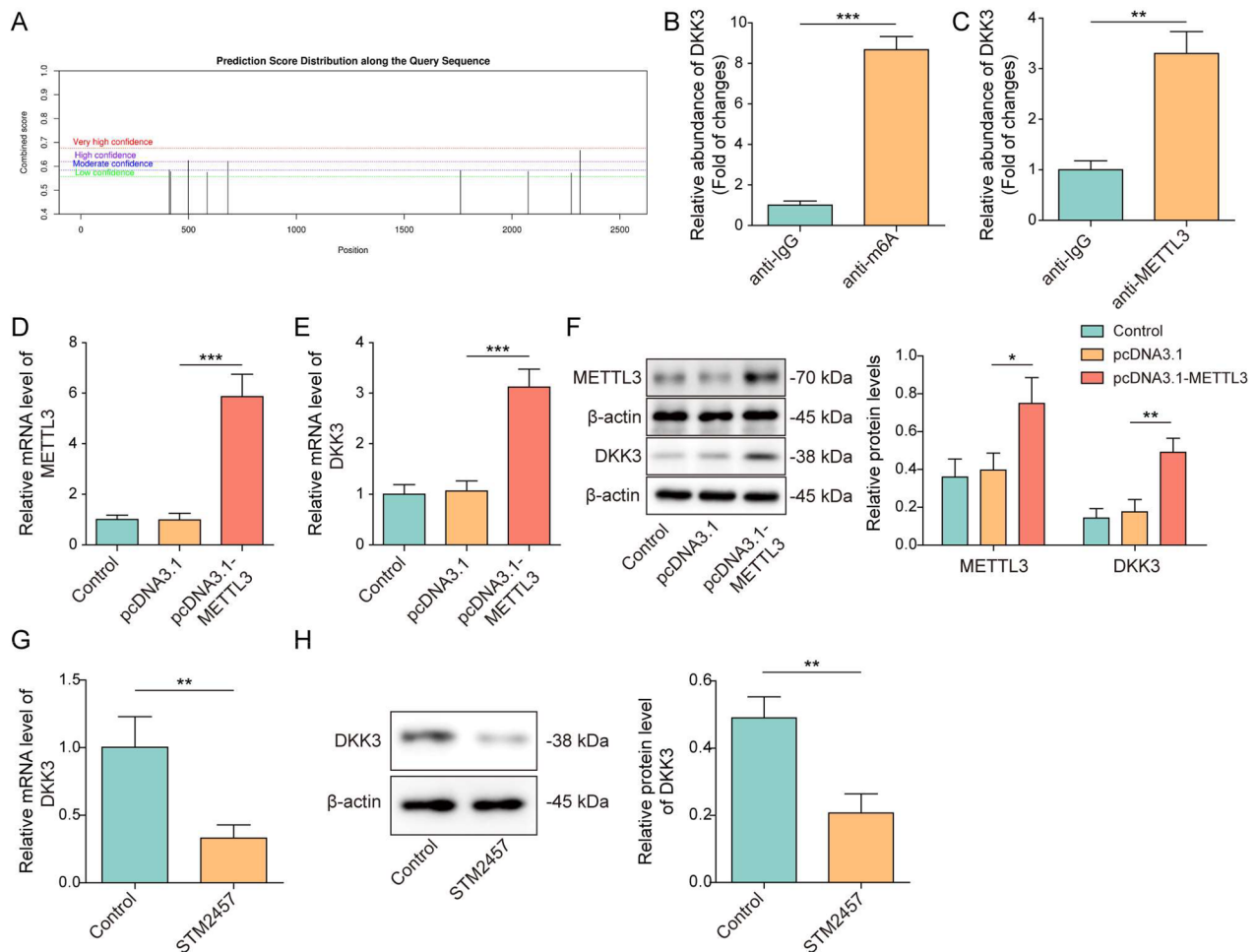

Figure 5. Upregulation of DKK3 was associated with METTL3-mediated m6A modification. A. Potential m6A sites on DKK3 mRNA were predicted by the SRAMP database. B. HK-2 cells were treated with H_2O_2. m6A level was detected by meRIP. C. The interaction between DKK3 and METTL3 was validated by RIP. HK-2 cells were treated with pcDNA3.1 or pcDNA3.1-METTL3. D&E. The mRNA levels of METTL3 and DKK3 were detected by qRT-PCR. F. The protein levels of METTL3 and DKK3 were detected by Western blotting. G&H. HK-2 cells were treated with STM2457 and the mRNA and protein level of DKK3 were detected by qRT-PCR and Western blotting, respectively. Data were presented as mean ± SD. *$p < 0.05$, **$p < 0.01$ and ***$p < 0.001$.
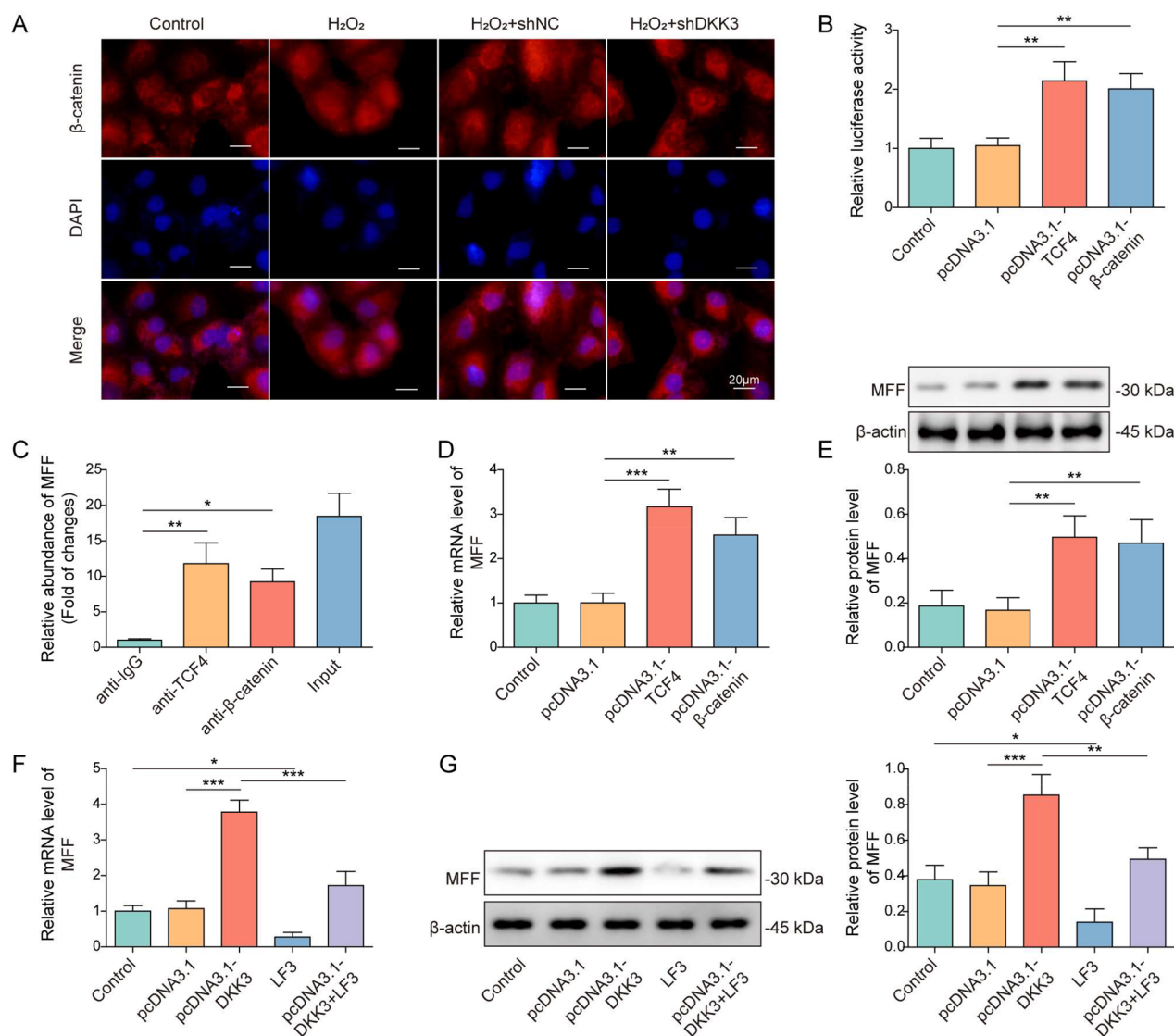
Figure 6. DKK3 promoted MFF transcription mediated by the TCF4/β-catenin complex. HK-2 cells transfected with shNC or shDKK3 were treated with saline (control group) or 500 μM H_2O_2 for 48 h. A. β-catenin was visualized by immunostaining. Scale bar, 20 μm. B. HK-2 cells were co-transfected with plasmids containing MFF's promoter or pcDNA3.1-TCF4/pcDNA3.1-β-catenin. The luciferase activity of treated cells was detected. C. ChIP was utilized to detect the interaction between TCF4, β-catenin and MFF promoter. IgG was used as the negative control. D. MFF mRNA was detected by qRT-PCR. E. MFF protein was detected by Western blotting. F. HK-2 cells were treated with saline (control), pcDNA3.1, pcDNA3.1-DKK3, LF3 or pcDNA3.1-DKK3+ LF3. MFF mRNA was detected by qRT-PCR. G. MFF protein was detected by Western blotting. Data were expressed as mean ± SD. *$p < 0.05$, **$p < 0.01$ and ***$p < 0.001$.

inhibitor) treatment (Figure 6(F&G)). Therefore, DKK3 stimulated TCF4/β-catenin complex-mediated MFF transcription.

MFF overexpression reversed the effect of DKK3 silencing on oxidative stress and mitochondrial homeostasis in H_2O_2-treated HK-2 cells

The role of MFF in DKK3-mediated oxidative stress and mitochondrial homeostasis of HK-2 cells was then investigated. The expression of MFF was markedly enhanced by pcDNA3.1-MFF, validating its efficiency (Figure 7(A)). CCK-8 assay showed that MFF overexpression counteracted the enhancement of cell viability caused by DKK3 suppression (Figure 7(B)). Additionally, MFF overexpression reversed DKK3 silencing's prevention of apoptosis in H_2O_2-induced HK-2 cells

(Figure 7(C)). Consistently, MFF overexpression reversed the effects of DKK3 silencing on Bcl2, Bax, and cleaved-caspase 3 (Figure 7(D)). The inhibitory impact of DKK3 silencing on mitochondrial ROS generation was reversed by MFF overexpression (Figure 7(E)). DKK3 silencing reduced the amount of MDA and increased the enzymatic activities of SOD and GPX in H_2O_2-induced HK-2 cells, and these effects were markedly reversed by MFF overexpression (Figure 7(F–H)). DKK3 silencing increased mitochondrial membrane potential in HK-2 cells exposed to H_2O_2, and MFF overexpression reverses this effect (Figure 7(I)). In H_2O_2-induced HK-2 cells, silencing of DKK3 increased the expression of mitochondrial fusion-related proteins Mfn2 and YME1L and inhibited the expression of NOX4 and mitochondrial fission genes MFF and Drp-1, and these regulatory effects were notably reversed by MFF
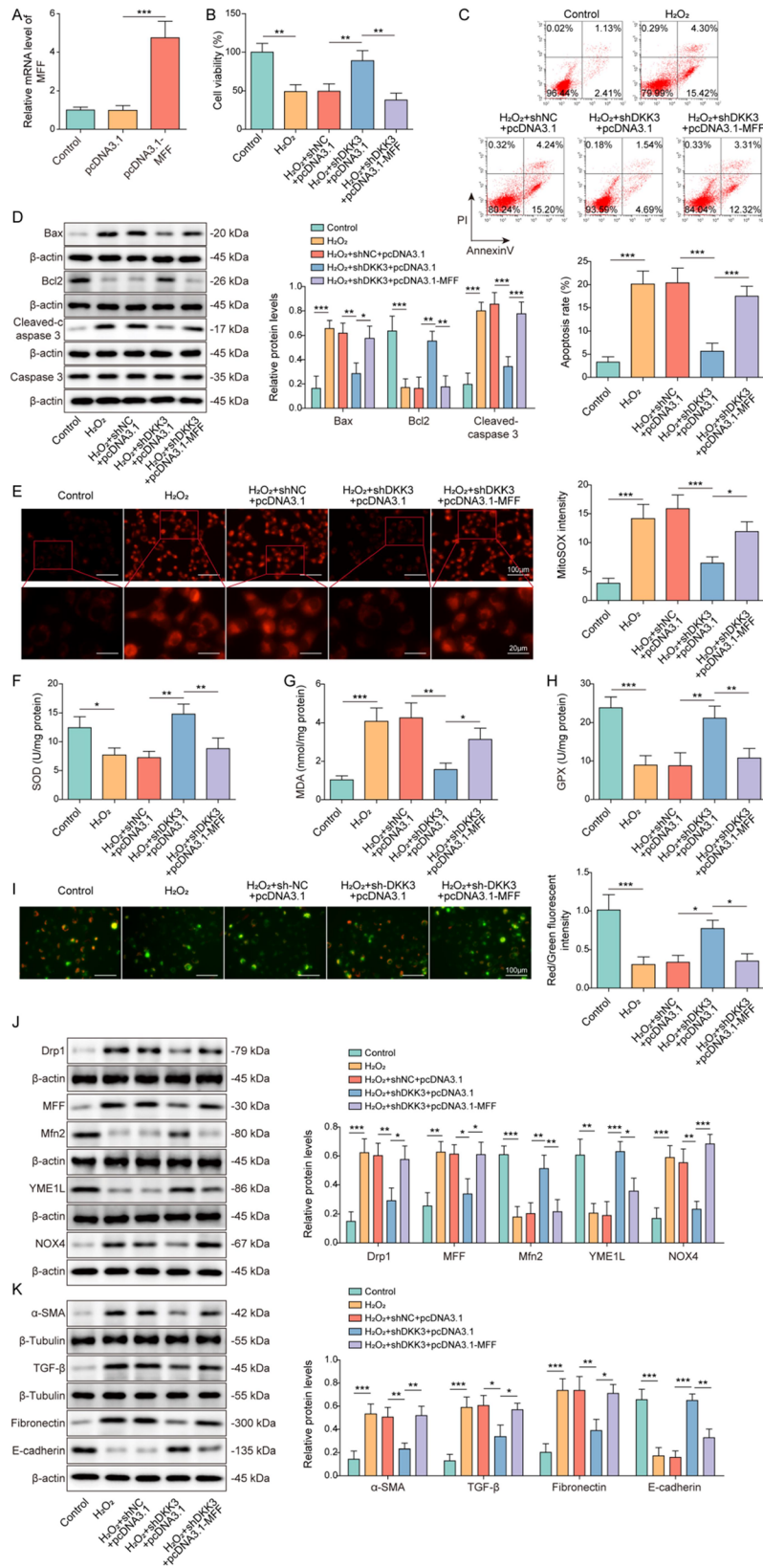
Figure 7. MFF overexpression reversed the effect of DKK3 silencing on biological activity in H_2O_2-treated HK-2 cells. A. MFF mRNA was detected by qRT-PCR in HK-2 cells transfected with pcDNA3.1-MFF. HK-2 cells were separated into the following groups: control, H_2O_2, H_2O_2+shNC+pcDNA3.1, H_2O_2+shDKK3+pcDNA3.1 and H_2O_2+shDKK3+pcDNA3.1-MFF. B. Cell viability was examined by CCK-8 assay kit. C. Cell apoptosis was assessed by flow cytometry. D. The protein expressions of Bax, Bcl2, Cleaved-caspase 3 and Caspase 3 in HK-2 cells were measured by Western blotting. E. Mitochondria ROS level was measured by mitoSOX assay kit. Scale bar, 100 μm and 20 μm. F. SOD was detected by the assay kit. G. MDA was detected by the assay kit. H. GPX was detected by the assay kit. I. Mitochondrial membrane potential was measured by the JC-1 detection kit. J. The protein expressions of Mfn2, MFF, Drp1, YME1L and NOX4 in HK-2 cells were measured by Western blotting. K. The protein expressions of α-SMA, Fibronectin, TGF-β and E-cadherin in HK-2 cells were measured by Western blotting. Data were expressed as mean±SD. *$p < 0.05$, **$p < 0.01$ and ***$p < 0.001$.
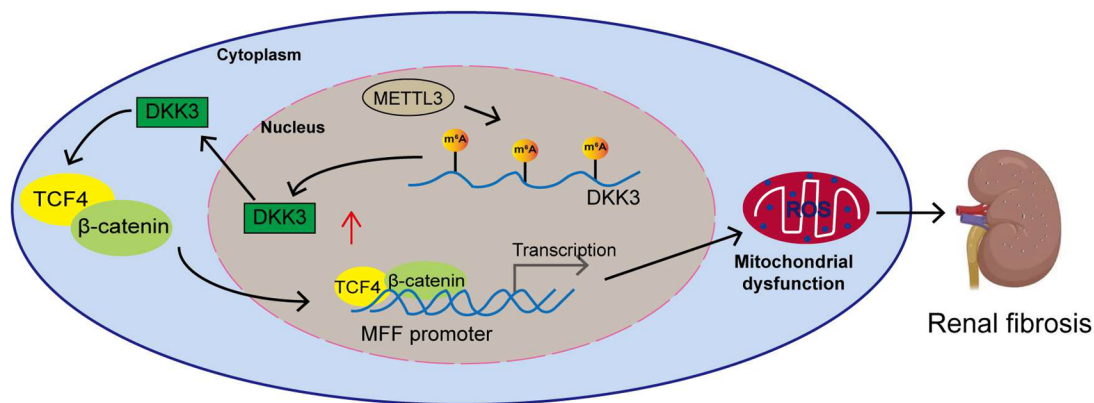
Figure 8. The molecular action schematic. METTL3 activates the DKK3-mediated TCF4/β-catenin signaling pathway by increasing the m6A modification on DKK3 and promotes the entry of TCF4 and β-catenin into the nucleus to increase MFF transcriptional expression, leading to mitochondrial dysfunction and oxidative stress, thereby causing renal fibrosis.

overexpression (Figure 7(J)). Silencing of DKK3 decreased the expression of fibrotic factors α-SMA, Fibronectin, and TGF-β and enhanced E-cadherin, and these effects were markedly restored following MFF overexpression (Figure 7(K)). Thus, MFF overexpression counteracted the effect of DKK3 silencing on oxidative stress and mitochondrial homeostasis.

Discussion

CKD is characterized by persistent renal tissue damage, resulting in irreversible impairment of renal function [26]. The detailed mechanism related to renal interstitial fibrosis is still unclear, and the current therapeutic efficacy is not very satisfactory. Therefore, it is necessary to grasp the pathophysiological mechanism of renal interstitial fibrosis and develop more ideal new treatments. Our studies demonstrated that knockdown of DKK3 suppressed oxidative stress, maintained mitochondria homeostasis, and inhibited cell apoptosis, thereby alleviated RF. Mechanistically, METTL3-mediated m6A modification elevated DKK3 in RF and then promoted MFF transcription *via* TCF4/β-catenin complex (Figure 8).

DKK3 participates in various biological processes such as cell differentiation, proliferation, and apoptosis, and plays an important role in tissue repair [27]. DKK3 reflects the dynamic process of renal tubular pressure injury and interstitial fibrosis and has the advantage of accurately identifying high-risk patients with short-term glomerular filtration rate (eGFR) decline [28]. Zewinger et al. [13] reported that urinary DKK3 could accurately identify high-risk patients with decreased eGFR and become a novel biomarker for monitoring the progression of CKD. The study of DKK3 in oxidative stress and mitochondria homeostasis was relatively limited. It was found that DKK3 promoted oxidative stress–induced fibroblast activity [29]. Moreover, the mechanisms of DKK3 in RF were much less examined. Our research found a novel role of DKK3 in the regulation of RF. DKK3 was highly expressed in both *in vitro* and *in vivo* RF models. Knockdown of DKK3 suppressed oxidative stress, maintained mitochondria homeostasis and inhibited apoptosis, thereby ameliorating the renal damage and fibrosis.

m6A is a methylation modification for adenylate N6 site, and its enzyme system includes methyltransferase, demethylase, etc. m6A modifications are involved in the regulation of RNA metabolism, including translation, splicing, degradation, etc., thereby regulating various cellular processes [30]. There are few studies on m6A modification in RF and CKD. METTL3 upregulated downstream genes by increasing the m6A modification level. For example, METTL3 enhanced CTSL mRNA stability through an m6A-IGF2BP2-dependent mechanism, thereby promoting cervical cancer cell metastasis [31]. METTL3 modulated m6A modification in UUO mice and promoted RF development by accelerating miR-21-5p maturation [18]. METTL3 could upregulate lncRNA transfer-associated lung adenocarcinoma transcript 1 (MALAT1) in obstructive nephropathy patients with RF through m6A modification, thereby promoting the viability, proliferation and migration of HK-2 cells [21]. Our study firstly discovered that METTL3 promoted DKK3 expression by increasing the m6A modification on DKK3.

DKK3 and Wnt signaling pathways function differently in different tissues [10]. Federico et al. [10] found that DKK3 mediated tubular atrophy and interstitial fibrosis by activating the Wnt pathway. Lipphardt et al. [11] found that DKK3 activated the Wnt signaling pathway by inhibiting the binding of DKK1 to LRP5/6. On the other hand, one study reported that increased expression of DKK3 was observed following prolonged exposure to albumin, contributing to inhibition of intracellular β-catenin signaling [32], indicating the function of DKK3 may be tissue-dependent. This study found that DKK3 activated Wnt signaling pathway by increasing the nuclear translocation of β-catenin in HK-2 cells. In UUO models, multiple members of the Wnt family were upregulated in damaged kidneys and β-catenin was persistently activated [33,34]. Sustained or uncontrolled Wnt/β-catenin signaling stimulated podocyte injury and proteinuria, ultimately leading to irreversible RF [12]. Additionally, Wnt/β-catenin signaling pathway is known to have regulatory role on mitochondria function [35,36]. Our study found that DKK3 promoted the transcriptional expression of MFF by facilitating β-catenin into the nucleus and activating β-catenin signaling pathway, which resulted in mitochondrial dysfunction in renal tubular epithelial cells. Our study reveals for the first time

that DKK3 mediated Wnt/β-catenin signaling regulates mitochondrial homeostasis through MFF.

MFF could control the division of mitochondria as well as regulate the morphology of peroxisomes. Therefore, MFF plays an important role in maintaining mitochondrial homeostasis [37]. The adaptor protein MFF plays a crucial role in facilitating the function of Drp1. Prior research has demonstrated that the activation of MFF is necessary for mitochondrial fission and oxidative damage to cardiac endothelial cells [38,39]. MFF simultaneously enhanced mitochondrial fission and inhibited Parkin-mediated mitophagy [40]. However, relatively few studies have been conducted on the role of MFF in RF. A study demonstrated that overexpression of NR4A1 could activate MFF-related mitochondrial fission, which caused oxidative stress and initiated mitochondria-dependent apoptosis [40]. No literature further characterized the role of MFF in RF. Our study found that DKK3 could activate the TCF4/β-catenin complex and increase MFF transcriptional expression. MFF overexpression could reverse the effects of DKK3 silencing on cellular biological functions, including apoptosis, oxidative stress response, and mitochondrial dysfunction.

In conclusion, we found that DKK3 was upregulated in RF, and knockdown of DKK3 alleviated kidney injury and fibrosis by inhibiting oxidative stress, apoptosis, and maintaining mitochondria homeostasis. Mechanistically, upregulation of DKK3 was regulated by METTL3-mediated m6A modification, which promoted MFF transcription mediated by the TCF4/β-catenin complex. Therefore, our work indicates that suppressing DKK3 may be a promising direction for treating RF.

Availability of data and material

All data generated or analyzed during this study are included in this published article.

References

[1] Ammirati AL. Chronic kidney disease. Rev Assoc Med Bras. 2020;66(suppl 1):1–16. doi: 10.1590/1806-9282.66.s1.3.

[2] Liu BC, Tang TT, Lv LL, et al. Renal tubule injury: a driving force toward chronic kidney disease. Kidney Int. 2018; 93(3):568–579. doi: 10.1016/j.kint.2017.09.033.

[3] Nakagawa S. [Identification of biomarkers for tubular injury and interstitial fibrosis in chronic kidney disease]. Yakugaku Zasshi. 2017;137(11):1355–1360. 2017/1/20 doi: 10.1248/yakushi.17-00150.

[4] Daenen K, Andries A, Mekahli D, et al. Oxidative stress in chronic kidney disease. Pediatr Nephrol. 2019; 34(6):975–991. doi: 10.1007/s00467-018-4005-4.

[5] Quadri MM, Fatima SS, Che RC, et al. Mitochondria and renal fibrosis. Adv Exp Med Biol. 2019; 1165:501–524. doi: 10.1007/978-981-13-8871-2_25.

[6] Kang HM, Ahn SH, Choi P, et al. Defective fatty acid oxidation in renal tubular epithelial cells has a key role in kidney fibrosis development. Nat Med. 2015;21(1):37–46. doi: 10.1038/nm.3762.

[7] Liu S, Soong Y, Seshan SV, et al. Novel cardiolipin therapeutic protects endothelial mitochondria during renal ischemia and mitigates microvascular rarefaction, inflammation, and fibrosis. Am J Physiol Renal Physiol. 2014;306(9):F970–80. doi: 10.1152/ajprenal.00697.2013.

[8] Otera H, Wang C, Cleland MM, et al. Mff is an essential factor for mitochondrial recruitment of Drp1 during mitochondrial fission in mammalian cells. J Cell Biol. 2010; 191(6):1141–1158. doi: 10.1083/jcb.201007152.

[9] Wang Y, Lu M, Xiong L, et al. Drp1-mediated mitochondrial fission promotes renal fibroblast activation and fibrogenesis. Cell Death Dis. 2020;11(1):29. doi: 10.1038/s41419-019-2218-5.

[10] Federico G, Meister M, Mathow D, et al. Tubular dickkopf-3 promotes the development of renal atrophy and fibrosis. JCI Insight. [Journal Article; Research Support, Non-U.S. Gov't]. 2016; 1(1):e84916. doi: 10.1172/jci.insight.84916.

[11] Lipphardt M, Dihazi H, Jeon NL, et al. Dickkopf-3 in aberrant endothelial secretome triggers renal fibroblast activation and endothelial-mesenchymal transition. Nephrol Dial Transplant. 2019; 34(1):49–62. doi: 10.1093/ndt/gfy100.

[12] Schunk SJ, Speer T, Petrakis I, et al. Dickkopf 3-a novel biomarker of the 'kidney injury continuum. Nephrol Dial Transplant. 2021;36(5):761–767. doi: 10.1093/ndt/gfaa003.

[13] Zewinger S, Rauen T, Rudnicki M, et al. Dickkopf-3 (DKK3) in urine identifies patients with Short-Term risk of eGFR loss. J Am Soc Nephrol. 2018;29(11):2722–2733. doi: 10.1681/ASN.2018040405.

[14] Jin Y, Murata H, Sakaguchi M, et al. Partial sensitization of human bladder cancer cells to a gene-therapeutic adenovirus carrying REIC/dkk-3 by downregulation of BRPK/PINK1. ONCOL REP. [Journal Article; Research Support, Non-U.S. Gov't]. 2012; 27(3):695–699.

[15] Takata A, Terauchi M, Hiramitsu S, et al. Dkk-3 induces apoptosis through mitochondrial and fas death receptor pathways in human mucinous ovarian cancer cells. Int J Gynecol Cancer. 2015; 25(3):372–379. doi: 10.1097/IGC.0000000000000340.

[16] Yang ZR, Dong WG, Lei XF, et al. Overexpression of dickkopf-3 induces apoptosis through mitochondrial pathway in human Colon cancer. World J Gastroenterol. 2012; 18(14):1590–1601. doi: 10.3748/wjg.v18.i14.1590.

[17] He H, Yuan K, Chen W. Effect of miR-25 on proliferation of nasopharyngeal carcinoma cells through wnt/beta-Catenin signaling pathway. Biomed Res Int. 2021;2021;2021::9957161. doi: 10.1155/2021/9957161.

[18] Liu E, Lv L, Zhan Y, et al. METTL3/N6-methyladenosine/miR-21-5p promotes obstructive renal fibrosis by regulating inflammation through SPRY1/ERK/NF-kappaB pathway activation. J Cell Mol Med. 2021; 25(16):7660–7674. doi: 10.1111/jcmm.16603.

[19] Han J, Wang J-Z, Yang X, et al. METTL3 promote tumor proliferation of bladder cancer by accelerating pri-miR221/222 maturation in m6A-dependent manner. Mol Cancer. 2019; 18(1):110. doi: 10.1186/s12943-019-1036-9.

[20] Zhang X, Li X, Jia H, et al. The m(6)a methyltransferase METTL3 modifies PGC-1alpha mRNA promoting mitochondrial dysfunction and oxLDL-induced inflammation in monocytes. J Biol Chem. 2021; 297(3):101058. doi: 10.1016/j.jbc.2021.101058.

[21] Liu P, Zhang B, Chen Z, et al. m(6)A-induced lncRNA MALAT1 aggravates renal fibrogenesis in obstructive nephropathy through the miR-145/FAK pathway. Aging (Albany NY). 2020; 12(6):5280–5299. doi: 10.18632/aging.102950.

[22] Li X, Pan J, Li H, et al. DsbA-L mediated renal tubulointerstitial fibrosis in UUO mice. Nat Commun. 2020;11(1):4467. doi: 10.1038/s41467-020-18304-z.

[23] Zhang D, Tu H, Cao L, et al. Reduced N-Type Ca(2+) channels in atrioventricular ganglion neurons are involved in ventricular arrhythmogenesis. J Am Heart Assoc. 2018; 7(2):e007457. doi: 10.1161/JAHA.117.007457.

[24] Xie L, Fu L, Mei C, et al. Icariin attenuates renal interstitial fibrosis through G protein-coupled estrogen receptor in a UUO murine model. Am J Transl Res. 2022; 14(3):1567–1577.

[25] Xuan MY, Piao SG, Ding J, et al. Dapagliflozin alleviates renal fibrosis by inhibiting RIP1-RIP3-MLKL-Mediated necroinflammation in unilateral ureteral obstruction. Front Pharmacol. 2021; 12:798381. doi: 10.3389/fphar.2021.798381.

[26] Chapman AB, Devuyst O, Eckardt K-U, et al. Autosomal-dominant polycystic kidney disease (ADPKD): executive summary from a kidney disease: improving global outcomes (KDIGO) controversies conference. Kidney Int. 2015; 88(1):17–27. doi: 10.1038/ki.2015.59.

[27] Li J, Zhou Z, Wen J, et al. Human amniotic mesenchymal stem cells promote endogenous bone regeneration. Front Endocrinol (Lausanne). 2020;11:543623. doi: 10.3389/fendo.2020.543623.

[28] Levin A, Tonelli M, Bonventre J, et al. Global kidney health 2017 and beyond: a roadmap for closing gaps in care, research, and policy. Lancet. 2017;390(10105):1888–1917. 2017/10/21 doi: 10.1016/S0140-6736(17)30788-2.

[29] Muecklich S, Shehzad K, Tiemann J, et al. DKK3 promotes oxidative stress–induced fibroblast activity. J Invest Dermatol. 2023;143(6):1088–1090.

[30] An Y, Duan H. The role of m6A RNA methylation in cancer metabolism. Mol Cancer. 2022; 21(1):14. doi: 10.1186/s12943-022-01500-4.

[31] Liu P, Ju M, Zheng X, et al. Methyltransferase-like 3 promotes cervical cancer metastasis by enhancing cathepsin L mRNA stability in an N6-methyladenosine-dependent manner. Cancer Sci. 2023; 114(3):837–854. doi: 10.1111/cas.15658.

[32] Wong DWL, Yiu WH, Wu HJ, et al. Downregulation of renal tubular wnt/beta-catenin signaling by dickkopf-3 induces tubular cell death in proteinuric nephropathy. Cell Death Dis. 2016; 7(3):e2155. doi: 10.1038/cddis.2016.62.

[33] He W, Dai C, Li Y, et al. Wnt/beta-catenin signaling promotes renal interstitial fibrosis. J Am Soc Nephrol. 2009; 20(4):765–776. doi: 10.1681/ASN.2008060566.

[34] Xiao L, Zhou D, Tan RJ, et al. Sustained activation of wnt/beta-Catenin signaling drives AKI to CKD progression. J Am Soc Nephrol. 2016; 27(6):1727–1740. doi: 10.1681/ASN.2015040449.

[35] Undi RB, Gutti U, Gutti RK. LiCl regulates mitochondrial biogenesis during megakaryocyte development. J Trace Elem Med Biol. 2017;39:193–201. doi: 10.1016/j.jtemb.2016.10.003.

[36] Yoon JC, Ng A, Kim BH, et al. Wnt signaling regulates mitochondrial physiology and insulin sensitivity. Genes Dev. 2010; 24(14):1507–1518. doi: 10.1101/gad.1924910.

[37] Passmore JB, Carmichael RE, Schrader TA, et al. Mitochondrial fission factor (MFF) is a critical regulator of peroxisome maturation. Biochim Biophys Acta Mol Cell Res. 2020; 1867(7):118709. doi: 10.1016/j.bbamcr.2020.118709.

[38] Jin Q, Li R, Hu N, et al. DUSP1 alleviates cardiac ischemia/reperfusion injury by suppressing the mff-required mitochondrial fission and Bnip3-related mitophagy via the JNK pathways. Redox Biol. 2018; 14:576–587. doi: 10.1016/j.redox.2017.11.004.

[39] Zhou H, Hu S, Jin Q, et al. Mff-Dependent mitochondrial fission contributes to the pathogenesis of cardiac microvasculature ischemia/reperfusion injury via induction of mROS-mediated cardiolipin oxidation and HK2/VDAC1 Disassociation-Involved mPTP opening. J Am Heart Assoc. 2017; 6(3):e005328.

[40] Sheng J, Li H, Dai Q, et al. NR4A1 promotes diabetic nephropathy by activating mff-mediated mitochondrial fission and suppressing Parkin-Mediated mitophagy. Cell Physiol Biochem. 2018; 48(4):1675–1693. doi: 10.1159/000492292.